

A Costimulatory CAR Improves TCR-based Cancer Immunotherapy



Bilal Omer^{1,2}, Mara G. Cardenas¹, Thomas Pfeiffer^{1,2}, Rachel Daum¹, Mai Huynh¹, Sandhya Sharma¹, Nazila Nouraei¹, Cicilyn Xie¹, Candise Tat¹, Silvana Perconti¹, Stacey Van Pelt¹, Lauren Scherer^{1,2}, Chris DeRenzo^{1,2,3}, Thomas Shum^{1,2}, Stephen Gottschalk^{1,2,3}, Caroline Arber^{1,4}, and Cliona M. Rooney¹

ABSTRACT

T-cell receptors (TCR) recognize intracellular and extracellular cancer antigens, allowing T cells to target many tumor antigens. To sustain proliferation and persistence, T cells require not only signaling through the TCR (signal 1), but also costimulatory (signal 2) and cytokine (signal 3) signaling. Because most cancer cells lack costimulatory molecules, TCR engagement at the tumor site results in incomplete T-cell activation and transient antitumor effects. To overcome this lack of signal 2, we genetically modified tumor-specific T cells with a costimulatory chimeric antigen receptor (CoCAR). Like classical CARs, CoCARs combine the antigen-binding domain of an antibody with costimulatory endodomains to trigger T-cell proliferation, but CoCARs lack the cytotoxic CD3 ζ chain to avoid toxicity to normal tissues. We first tested a CD19-targeting CoCAR in combination with an HLA-A*02:01-restricted,

survivin-specific transgenic TCR (sTCR) in serial cocultures with leukemia cells coexpressing the cognate peptide–HLA complex (signal 1) and CD19 (signal 2). The CoCAR enabled sTCR⁺ T cells to kill tumors over a median of four additional tumor challenges. CoCAR activity depended on CD19 but was maintained in tumors with heterogeneous CD19 expression. In a murine tumor model, sTCR⁺CoCAR⁺ T cells improved tumor control and prolonged survival compared with sTCR⁺ T cells. We further evaluated the CoCAR in Epstein–Barr virus–specific T cells (EBVST). CoCAR-expressing EBVSTs expanded more rapidly than nontransduced EBVSTs and delayed tumor progression in an EBV⁺ murine lymphoma model. Overall, we demonstrated that the CoCAR can increase the activity of T cells expressing both native and transgenic TCRs and enhance antitumor responses.

Introduction

Adoptive cell therapy (ACT) with T cells expressing either native or transgenic T-cell receptors (TCR) is an attractive immunotherapeutic approach because of the large diversity of antigens that can be targeted (1). *Ex vivo*–expanded, polyclonal T-cell therapies, in which T cells express native (n)TCRs, can be specific for multiple epitopes from multiple tumor antigens, overcoming the problem of tumor heterogeneity. Epstein–Barr virus (EBV)-specific T cells (EBVST) have proven successful against EBV-associated malignancies, as have

tumor-infiltrating lymphocytes (TIL) for melanoma and other solid tumors (2–6). Transgenic TCR-based (tTCR) T-cell therapies can efficiently redirect polyclonal T cells to a defined peptide–HLA complex with high reproducibility and defined affinity. These tTCR⁺ T cells have achieved promising clinical results against several tumor antigens expressed in melanoma, myeloma, synovial sarcoma, and acute myeloid leukemia (7–12). However, limited persistence and immune suppression in the tumor microenvironment (TME) are major causes for treatment failure with both treatments (11).

Clinical responses and T-cell persistence are correlated in both nTCR and tTCR therapies (2, 9). Unlike chimeric antigen receptor (CAR) T cells, which target cell surface antigens and are engineered with built-in costimulation, TCRs target immunogenic peptides presented on the cell surface in the context of MHC molecules. Therefore, TCRs rely on naturally occurring, host derived costimulation and cytokine signals (12). In the immunosuppressive TME, many factors impair tumor-specific T-cell function and persistence (11). Most tumors lack costimulatory ligands and inhibit professional antigen-presenting cells that normally present antigen in an immunostimulatory context.

For this study, we engineered CD19-targeting, costimulatory CARs (CoCAR) that lacked the cytotoxic ζ chain of conventional CARs, but still provide T-cell costimulation upon CD19 ligation in the TME of hematologic malignancies (i.e., bone marrow, lymphatic system, blood). CD19 is a well-characterized target for conventional CARs, and for the CoCAR, we selected a single-chain variable fragment (scFv) derived from a CD19-CAR that has been clinically tested (13). In this CD19-CoCAR model system, we confirmed the lack of CoCAR toxicity on target antigen-positive cells by demonstrating the absence of B-cell killing. We created CoCARs with three different costimulatory endodomains to optimize their costimulatory capacity and cytotoxicity was conferred only via the TCR. We validated the CoCAR approach in two model systems: a tTCR targeting an immunodominant epitope of survivin, which is overexpressed in leukemia (14–16),

¹Center for Cell and Gene Therapy, Texas Children's Hospital, Houston Methodist Hospital, Baylor College of Medicine, Houston, Texas. ²Texas Children's Cancer and Hematology Centers, Texas Children's Hospital, Baylor College of Medicine, Houston, Texas. ³Department of Bone Marrow Transplant and Cellular Therapy, St. Jude's Children's Research Hospital, Memphis, Tennessee. ⁴Department of Oncology UNIL-CHUV, Lausanne University Hospital, University of Lausanne and Ludwig Institute for Cancer Research Lausanne, Epalinges, Switzerland.

Note: Supplementary data for this article are available at Cancer Immunology Research Online (<http://cancerimmunolres.aacrjournals.org/>).

C. Arber and C.M. Rooney contributed as co-senior authors to this article.

Corresponding Authors: Bilal Omer, Pediatrics, Center for Cell and Gene Therapy, Baylor College of Medicine/Texas Children's Hospital/Houston Methodist Hospital, 1102 Bates Ave, Houston, TX 77030. Phone: 183-2824-6855; Fax: 183-2825-4732; E-mail: bomer@bcm.edu; and Caroline Arber, Department of Oncology UNIL-CHUV, Lausanne University Hospital, University of Lausanne and Ludwig Institute for Cancer Research Lausanne, Chemin des Boveresses 155, CH-1066 Epalinges, Switzerland. E-mail: caroline.arber@unil.ch

Cancer Immunol Res 2022;10:512–24

doi: 10.1158/2326-6066.CIR-21-0307

This open access article is distributed under Creative Commons Attribution-NonCommercial-NoDerivatives License 4.0 International (CC BY-NC-ND).

©2022 The Authors; Published by the American Association for Cancer Research

and nTCR-based, polyclonal EBVSTs to target EBV⁺ lymphoma (17). In both model systems, CoCAR⁺ T cells had enhanced persistence and antitumor activity, an effect maintained even in tumors with heterogeneous CoCAR target antigen expression.

Materials and Methods

Human samples and cell lines

Peripheral blood was obtained from HLA-typed (HLA-A2⁺) healthy donors under a Baylor College of Medicine (BCM) Institutional Review Board–approved protocol. Informed written consent was obtained from all donors, and research was guided by the Declaration of Helsinki, the International Ethical Guidelines for Biomedical Research Involving Human Subjects (CIOMS), Belmont Report, and U.S. Common Rule. Peripheral blood mononuclear cells (PBMC) were separated using Lymphoprep solution (Stemcell Technologies, 07801).

BV173 cells (B-cell acute lymphoblastic leukemia) were obtained from German Cell Culture Collection (DSMZ, #ACC 20, obtained and frozen by C. Arber) and maintained in RPMI1640 medium (Hyclone, SH3002701) supplemented with 20% FBS (Hyclone, 10-082-139) and 2 mmol/L GlutaMAX (Invitrogen 35050-061). A CD19-knockout (KO) BV173 line was generated by CRISPR/Cas9 as described previously (18). In brief, two CD19-specific single-guide RNAs (5'-ttaatacactactataGGGCCCAAGCTGTATGTGTgttttag-agctagaatagc-3' and 5'-ttaatacactactataGGGACCCATGTGCAC-CCCAAGtttagactagaatagc-3') and a recombinant Cas9 protein (CP01, PNA Bio) were used. 1 µg of each was mixed at room temperature and used to electroporate 0.15 × 10⁶ BV173 cells (three pulses of 1,600 V for 10 ms, Neon Transfection System, Invitrogen). Electroporated cells were expanded in antibiotic-free medium as above, and CD19-negative cells were sorted to greater than 98% purity. A beta-2-microglobulin (B2M)-KO BV173 cell line was generated as previously described and provided by C. Arber (16). Knockout was confirmed by staining with HLA antibodies (Thermo Fisher Scientific, #11-9983-42). BV173 cells stably expressing firefly luciferase (FFLuc) from a retroviral vector were generated as described previously (14) and maintained in RPMI medium with 100 µg/mL geneticin (Gibco, 14072). 293T cells for transfection were obtained from the ATCC (#CRL-3216) and maintained in Iscove's modified Dulbecco's medium (#12440054, Thermo Fisher Scientific) supplemented with 10% FBS and 2 mmol/L GlutaMAX. Cells were expanded for one passage after thawing.

EBV-transformed lymphoblastoid cell lines (LCL) were generated from healthy donor PBMCs by incubation with supernatant from the B95-8 EBV producer cell line (provided by C.M. Rooney), in the presence of 1 µg/mL cyclosporine A (Sandoz), and then maintained in RPMI1640 medium supplemented with 10% FBS and 2 mmol/L GlutaMAX (19). CEM-T2 (TAP transporter-deficient) cells were obtained from the ATCC. All cell lines were *Mycoplasma* free.

Retroviral vector construction and production

A retroviral vector expressing the survivin T-cell receptor (sTCR) has been described previously (14) and was provided by C. Arber. Briefly, the TCR α and β chains of a T-cell clone specific for the human HLA-A*0201-restricted survivin 95–104 (ELT) epitope were codon optimized by GeneArt (Invitrogen) and cloned into a retroviral vector after replacement of the constant regions with the corresponding murine regions (Fig. 1A). To generate the CD19-CoCAR vector, the CD19-specific FMC63 scFv (20) was cloned in-frame into SFG retroviral vectors [provided by C.M. Rooney (13)]

encoding a short Fc hinge and a CD28-derived transmembrane domain with CD28.OX40-, CD28-, or 4-1BB-derived costimulatory endodomains: CD19.28 (CoCAR1), CD19.41BB (CoCAR2), and CD19.28-OX40 (CoCAR3). The CoCAR constructs also contained an IRES sequence, followed by a truncated nerve growth factor receptor (NGFR; ΔCD271) as a detection marker (Fig. 1A). NGFR was introduced into vectors by In-Fusion cloning (Takara Bio In-Fusion HD Cloning Kit, # 639649). Retroviral vector supernatants were produced by transient cotransfection of 293T cells with (i) the plasmids of interest (with LTRs and packaging signals), (ii) the Peg-Pam plasmid encoding MoMLV gag-pol, and (iii) the RDF plasmid encoding the RD114 envelope using GeneJuice transfection reagent (EMD Millipore Corp) as described previously (21). At 48 and 72 hours posttransfection, retroviral supernatant was collected, filtered using a 0.45-µm filter (PALL Life Sciences, #4654), snap frozen, and stored at –80°C.

Generation of activated T cells

CD8⁺ T cells were isolated from fresh healthy donor PBMCs of HLA-A2⁺ donors with CD8 magnetic-activated cell sorting (MACS) beads (130-045-201, Miltenyi Biotec GmbH; purity >90%). One million CD8⁺ T cells were stimulated for 3 days in nontissue culture-treated, 24-well plates (Falcon, catalog no. 351147) coated with anti-CD3 produced in-house by the OKT3 hybridoma (ATCC catalog no. CRL-8011, RRID:CVCL_DC77) and anti-CD28 (BD Biosciences, catalog no. 348040, RRID:AB_400367, clone L293), each at 1 µg/mL. ATCs were maintained in T-cell medium consisting of a 1:1 mixture of RPMI1640 and Click's medium (Fujifilm Irvine Scientific, 92705), 10% human AB serum (Valley Biomedical), and 2 mmol/L GlutaMAX (Thermo Fisher Scientific, #35050061). The cells were supplemented with IL7 and IL15 (R&D Systems, 204-IL), both at 10 ng/mL, every 3 days and split as needed.

Preparation of DCs

Dendritic cells (DC) were generated for the initiation of EBVST cultures by isolating monocytes from fresh healthy donor PBMCs with CD14 MACS beads (Miltenyi Biotec; purity >90%). CD14⁺ monocytes were cultured in DC media (CellGenix, 20801-0500), supplemented with 800 U/mL GM-CSF (Thermo Fisher Scientific, PHC2011) and 1,000 U/mL of IL4 (R&D Systems, 204-IL) for 5 days, with GM-CSF and IL4 replenishment on day 3. DCs were matured on day 5 with 10 ng/mL IL1β, 100 ng/mL of IL6, 10 ng/mL of TNFα (R&D Systems), 1 µg/mL of PGE-2 (Sigma), 400 IU/mL of IL4, and 800 IU/mL GM-CSF as described previously (22) and cultured for 2 additional days before harvest.

Generation of EBVSTs and irrelevant cytomegalovirus-specific T cells

Fresh healthy donor PBMCs were depleted of naïve CD45RA⁺ T cells using CD45RA MACS beads (130-045-901, Miltenyi Biotec; ref. 23) to isolate memory T cells for EBVST or cytomegalovirus-specific T cell (CMVST) generation. Autologous mature DCs were pulsed at 37°C for 1 hour with 1 ng/mL EBV pepmixes (JPT Peptide Technologies) comprising 15-mer amino acid peptides that overlapped by 11 amino acids and covered the entire protein sequence of IE-1 and pp65 for the CMVST controls and the EBV latent antigens EBNA1, LMP1, and LMP2 for the EBVSTs (17). Memory T cells were then plated with the EBV or CMV pepmix-pulsed DCs at a PBMC:DC ratio of 20:1 in a 24-well tissue culture plate. The stimulated memory T cells were fed with 10 ng/mL of IL7 and IL15, transduced with the retroviral vector on day 3, and supplemented with cytokines every 2 to

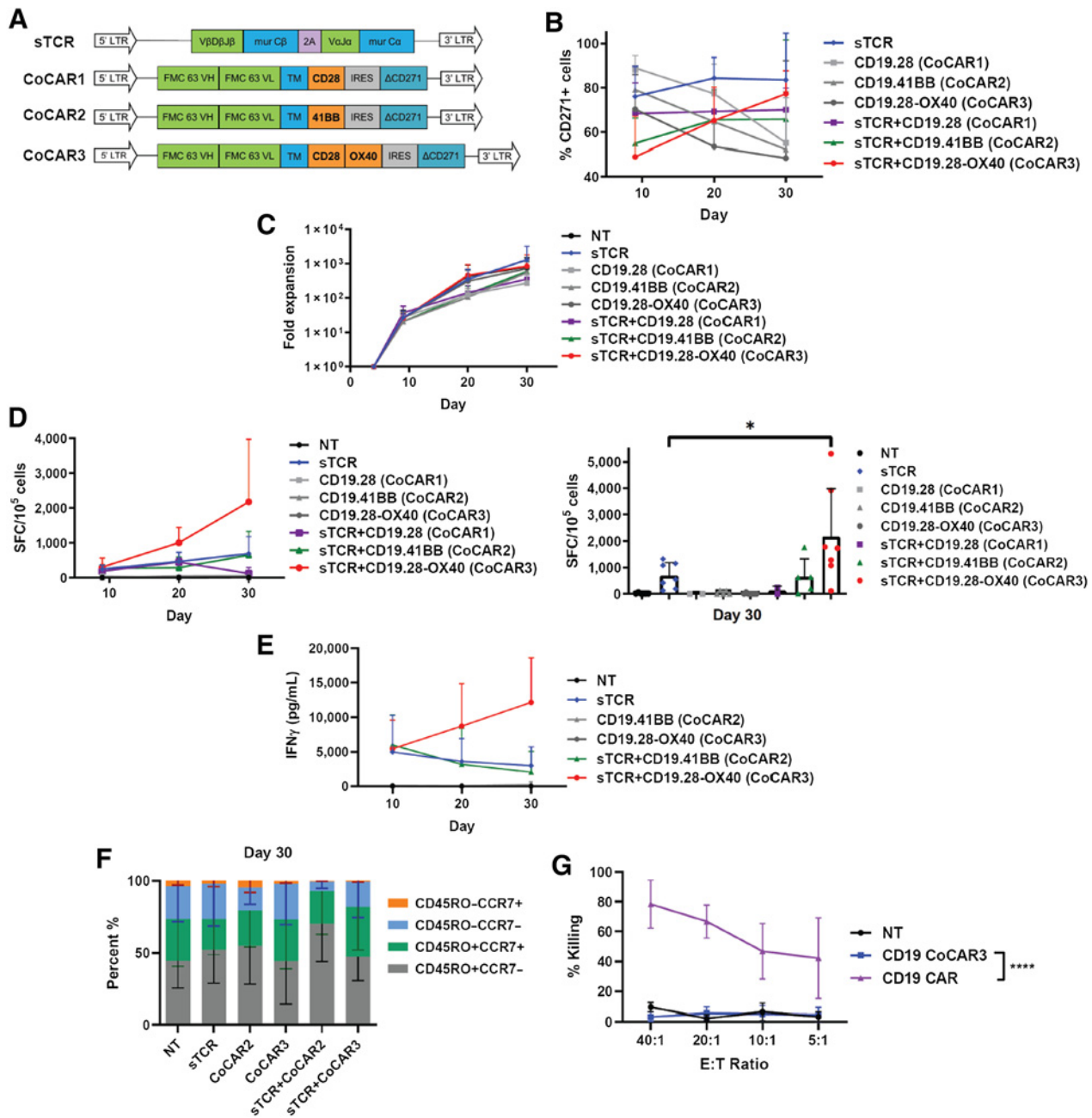


Figure 1.

CoCAR3 enhances antigen sensitivity of sTCR⁺ T cells. **A**, Schematic of retroviral vectors encoding the sTCR and CoCAR1-3. CoCAR1-3 are fusion proteins consisting of an anti-CD19 scFv (FMC63), CD28 transmembrane domain, and costimulatory endodomains. For detection and selection, the vectors contained an IRES followed by a truncated NGFR (Δ CD271). LTR, long terminal repeat; VH, variable region of heavy chain; VL, variable region of light chain. **B**, Frequency of transgenic (CD271⁺) T cells in culture with weekly antigen-specific stimulations (see Materials and Methods; CoCAR1⁺ and sTCR⁺CoCAR1⁺ T cells, $n = 3$; CoCAR2⁺ and sTCR⁺CoCAR2⁺ T cells, $n = 5$; others, $n = 7$). **C**, Fold expansion after transduction and following weekly stimulations (see Materials and Methods; $n = 7$). **D**, Frequency of IFN γ spot-forming cells (SFC) in response to survivin-peptide pulsed T2 cells by ELISpot ($n = 6$) over time (left) and separately at day 30 (right). **E**, Total IFN γ secretion in response to survivin-peptide pulsed T2 cells by ELISA ($n = 7$ day 10, $n = 6$ day 20, and $n = 4$ day 30). **F**, Memory phenotype of T cells defined by CD45RO and CCR7 expression (day 30, $n = 5$). **G**, 4-hour ⁵¹chromium-release cytotoxicity assay with NT, single-transduced CoCAR⁺, and single-transduced CD19-CAR⁺ T cells against B cells at the E:T ratios shown ($n = 5$). **C-E**, NT: nontransduced T cells. **B-G**, mean \pm SD; “ n ” denotes the number of individual healthy donors. Statistical significance was determined by Tukey test (**D**) and ANOVA (area under the curve; **G**), *, $P < 0.05$; ****, $P < 0.0001$.

3 days throughout the culture. A second stimulation with pepmix-pulsed autologous irradiated PBMCs at a ratio of 1:1 was performed between days 9 and 11. A third stimulation with pepmix-pulsed irradiated PBMCs occurred 7 to 9 days following the second stimulation. Functional assays were performed on the days of each restimulation and 7 days after the third stimulation.

Transduction of EBVSTs and ATCs

ATCs or EBVSTs were transduced 3 days after activation. The day prior to transduction, 24-well, nontissue culture plates were coated with 3.5 μg of RetroNectin (Takara T100B; RetroNectin concentration 7 $\mu\text{g}/\text{mL}$) in 0.5 mL of Dulbecco's PBS (Sigma-Aldrich, D8537) and kept at 4°C overnight. Following RetroNectin removal, 1 mL of retroviral supernatant containing either sTCR or CoCAR encoding retroviral particles was added to each well. For generation of sTCR⁺CoCAR⁺ ATCs or EBVSTs, 1 mL of each retroviral supernatant was mixed and added to each well. Conventional CD19-CAR ATCs were generated by adding 1 mL of retroviral supernatant containing the CD19-CAR encoding retroviral particles (13) to each well. The plates were then centrifuged at 2,000 $\times g$ for 1 hour at 4°C to promote viral adhesion to the RetroNectin. Following centrifugation, the supernatant was aspirated and 2 $\times 10^5$ T cells were added to each well in T-cell medium with 10 ng/mL IL7 and IL15. The plates were incubated at 37°C for the following 2 to 3 days before collection and replating in fresh T-cell medium. ATCs were expanded for 6 to 7 days prior to initiation of functional assays, with supplementation of 10 ng/mL IL7 and IL15 every 3 days. EBVSTs were expanded as described above. For the *in vivo* experiment, another transduction, as described above, was performed with GFP-firefly luciferase 3 days after the second stimulation.

Cytotoxicity assay

Chromium release cytotoxicity assays were performed against target B cells. A total of 1 $\times 10^6$ B cells (LCLs as described above) were incubated with ⁵¹Cr sodium chromate (PerkinElmer) at 37°C for 1 hour and then washed with T-cell medium as above. The following effector cells were used at multiple effector to target cell ratios (20:1, 10:1, 5:1, 2.5:1): nontransduced (NT) ATCs, CoCAR-transduced ATCs, and conventional CD19-CAR ATCs (13). Effector and target cells were cocultured in 96-well plates for 4 hours. Target cells cultured without effector cells or lysed with 0.1% Triton-X (Sigma-Aldrich, #T8787) served as the controls for spontaneous release and maximum release, respectively. Cytotoxicity against B cells was assessed by the amount of chromium released (counts per minute, CPM), as quantified by a gamma counter (PerkinElmer 2470 WIZARD2). Specific lysis percentage was calculated by subtracting the spontaneous release from the measured CPM and then dividing by the difference of the maximum release and the spontaneous release.

Flow cytometry

We measured transduction efficiencies by flow cytometry and used NT cells as negative controls. Cells were washed in PBS, then the appropriate detection antibodies were added to 2.5 $\times 10^5$ pelleted cells and incubated for 20 minutes in the dark at room temperature. The cells were then washed in PBS and analyzed on a Gallios flow cytometer (Beckman Coulter 10 color/3 laser). All analysis was conducted with Kaluza Analysis Software (Beckman Coulter). Antigen presenting cell (APC)-conjugated antibody to the constant region of the TCR β -chain was used to detect sTCR (Invitrogen, #14-5961-82, clone H57-597) and PE- or BV421-conjugated CD271 was used for detecting the CoCAR (BD #562562, clone C40-1457).

For coculture assays, ATCs were identified using APC 700-conjugated CD8 antibody (Beckman Coulter, catalog no. A66332, RRID:AB_2750854, clone B9.11), and BV173 target cells were detected with FITC-conjugated anti-CD33 (BD #555626, clone HIM3-4). Cells were phenotyped with BV421-conjugated anti-CCR7 (#353207, clone G043H7) and ECD-conjugated anti-CD45RO (Beckman Coulter #IM2712U, clone UCHL1) to assess memory phenotype. Anti-TIM-3 (FITC; F38-2E2, Thermo Fisher Scientific), anti-LAG3 (#369212, BioLegend), and anti-PD-1 (PC7, #A78885, Beckman Coulter) were used for analysis of markers of T-cell exhaustion.

The initial gate for all analysis was set on lymphocytes using SSC and FSC. A gate was then placed on CD8⁺ cells to characterize CD8⁺ T cells. For coculture assays, an additional gate was set on CD33⁺ cells to identify tumor cells.

Enzyme-linked immunospot assay

We used enzyme-linked immunospot (ELISpot) analysis to quantify the number of cells secreting IFN γ in response to appropriate antigen stimulation. A total of 1 $\times 10^5$ effector cells were plated in triplicate in a 96-well plate precoated overnight with immobilized anti-IFN γ (MabTech, #3420-3-1000) at 10 $\mu\text{L}/\text{mL}$ as described previously (24). T2 cells pulsed with 1 μL of survivin peptide (0.1 mol/L) were used as target cells for experiments using sTCR⁺ and sTCR⁺CoCAR⁺ cells. EBVSTs and CoCAR⁺ EBVSTs were directly pulsed with EBV pepmixes (1 $\mu\text{g}/\text{mL}$) or medium alone. Following overnight incubation at 37°C, cells were removed, and the plates were developed with anti-IFN γ (MabTech, #3420-6-5000 at 1 $\mu\text{L}/\text{mL}$), dried overnight, and sent to ZellNet Consulting for quantification. To control for background signal, the number of spot-forming cells of the negative control was subtracted from those of the experimental conditions.

In vitro cocultures

ATCs from four different conditions (NT, sTCR alone, CoCAR alone, or sTCR⁺CoCAR⁺) were serially cocultured with tumor cells to measure their antitumor efficacy at an effector to target (E:T) ratio of 1:5. ATCs were plated in 48-well tissue culture plates at 1 $\times 10^5$ cells per well in multiple replicates. Wild-type (WT), CD19 knockout (CD19-KO), or B2M-KO BV173 cells were added at 5 $\times 10^5$ cells per well in T-cell medium. No supplemental cytokines were added. Every 3 to 4 days, for up to eight rounds of serial cocultures, a single well was harvested for flow cytometry to quantify remaining BV173 tumor cells and T cells. The same day, 5 $\times 10^5$ fresh BV173 cells were added to the remaining wells. To determine whether CD19 was required on all target cells, a serial coculture assay was performed using decreasing ratios of WT to CD19-KO BV173 target cells as indicated in figures. The E:T-cell ratio of 1:5 was maintained throughout all rounds of coculture, but the ratio of WT to CD19-KO BV173 cells was varied as specified in the figure legends. Supernatants were collected for IFN γ analysis via ELISA as described below. The experimental endpoint for the cocultures was defined as failure of the T cells to eliminate the tumor cells.

ELISAs

IFN γ ELISAs were performed as directed by the manufacturer's protocol (R&D Systems, #DIF50) to quantify amounts of IFN γ in supernatants from the cocultures described above. Supernatants were harvested 24 hours after the addition of fresh BV173 cells. IFN γ secreted was quantified by the absorbance of anti-IFN γ conjugated to horseradish peroxidase at 450 nm (Tecan InfiniteF50). To convert

absorbance to concentration, manufacturer provided IFN γ standards of known concentrations were used to create a standard curve.

Metabolic assays

WT BV173 cells were cocultured with either sTCR⁺ or sTCR⁺CoCAR3⁺ T cells at an E:T ratio of 1:5 for two rounds of serial coculture as described above. T cells were collected, mixed with BV173 cells at a ratio of 1:5 for 24 hours, and then separated using CD4 and CD8 MACS beads (Miltenyi Biotec, Germany, #130-045-101 and 130-045-201). Mitochondrial function was determined using Agilent Seahorse XFe96 Extracellular Flux Assay Kits (Agilent, catalog no. 102416), and analysis was conducted by the Baylor College of Medicine Mouse Metabolic and Phenotyping Core. Data were analyzed using the Seahorse Wave software (ECAR and OCR/Agilent).

Gene expression analysis using NanoString

WT BV173 cells were cocultured with either sTCR⁺ or sTCR⁺CoCAR⁺ ATCs at an E:T ratio of 1:5. Four days later, flow cytometry was performed to measure tumor elimination, and 5×10^5 BV173 cells were added back per well of culture. Twenty-four hours later, the cocultured cells were harvested. In conditions in which BV173 cells were still present, CD33 MACS beads (130-045-501, Miltenyi Biotec) were used to deplete residual tumor cells. Total RNA was collected from ATCs using the RNeasy Micro Kit (Qiagen) following kit instructions for extraction from cells. Gene expression analysis (NanoString) was performed by the Baylor College of Medicine Genomic and RNA Profiling Core using the nCounter CAR-T Characterization Panel. Submitted samples were >250 ng and <5 μ L. Data were analyzed using the nSolver 3.0 software (NanoString). See statistical section for additional information on NanoString analysis.

In vivo mouse xenograft models

Animal experiments were conducted on a protocol approved by BCM's Institutional Animal Care and Use Committee. To test the antitumor activity of sTCR⁺CoCAR⁺ ATCs *in vivo*, 3×10^6 BV173-FFLuc cells were injected intravenously into the tail vein of female NOD SCID γ c^{-/-} (NSG; Jackson Labs) mice after irradiating mice at 120cGy (Precision XRad320). After the indicated timeframe, ATCs (NT, sTCR⁺, CoCAR⁺, or sTCR⁺CoCAR⁺) at the indicated dose were injected into the tail vein. Tumor signal was measured by bioluminescent imaging (BLI; Xenogen, IVIS, Small Animal Core Facility, Texas Children's Hospital), beginning 1 week after T-cell injection and continuing weekly thereafter. To prepare for BLI, mice were anesthetized with isoflurane (USP, Covetrus, OH #029405) then injected with luciferin (PerkinElmer, #122799) intraperitoneally. After 10 minutes, mice were placed in the IVIS for imaging. Mice were euthanized if they had impaired mobility or had >20% body weight loss. To measure the effect of the CoCAR on EBVSTs, 3×10^6 EBV-LCLs were injected subcutaneously into NSG mice. A total of 5×10^6 FFLuc+ EBVSTs or irrelevant CMVSTs (control) were injected the following day. EBVST bioluminescence signal was measured weekly by BLI, and tumor volume was measured with a digital caliper (Whitworth 0–150 mm) weekly. Mice were euthanized when tumors reached 1.5 mm diameter in the longest axis. Tissue was collected at the experimental endpoint or at times of early euthanasia. All mice were purchased from Jackson Laboratories.

Statistical analysis

Descriptive statistics with mean and SDs were used to summarize results. Student *t* test or ANOVA, when appropriate, was used to test for significance between different conditions in each assay. A *P* value < 0.05 was considered statistically significant. Survival for

in vivo experiments was analyzed by the Kaplan–Meier method, and survival differences were compared using the log-rank test. NanoString data were analyzed using the nSolver 3.0 software and the “Advanced Analysis” function with standard normalization; *P*-value cutoff was set at *P* = 0.05, and the Benjamini–Hochberg correction was applied.

Results

CoCAR3 enhances expansion and antigen sensitivity of tTCR T cells

To identify the optimal signaling domain(s) for our CoCAR strategy, we tested three CoCAR constructs with different costimulatory endodomains: CD19.28 (CoCAR1), CD19.41BB (CoCAR2), and CD19.28-OX40 (CoCAR3). All constructs included truncated NGFR/CD271 (Δ CD271) as a transduction marker (Fig. 1A). To assess their costimulatory capacity *in vitro*, we coexpressed the CoCARs with a transgenic HLA-A*02:01-restricted TCR targeting the tumor-associated antigen survivin (sTCR; Fig. 1A; ref. 14). NT, single-transduced (sTCR⁺ or CoCAR⁺), and double-transduced (sTCR⁺CoCAR⁺) CD8⁺ T cells were expanded using three antigen-specific stimulations, and autologous, PBMC that contain a fraction of normal CD19⁺ B cells. T-cell expansion, transgene expression, and antigen-specific IFN γ production during expansion was assessed. The dual-transgenic population was enriched in the sTCR⁺CD19.28-OX40⁺ condition from 49% (\pm 18.1) to 77% (\pm 10.4, *P* < 0.01) between days 9 and 30, whereas the proportion of transgenic cells remained stable in sTCR⁺, sTCR⁺CD19.41BB⁺, and sTCR⁺CD19.28⁺ T cells (Fig. 1B). In contrast, T-cell cultures transduced with any of the three CoCARs alone showed a nonsignificant decrease in transgene-expressing cells over time. T-cell expansion was overall comparable across conditions (Fig. 1C). By the end of the third stimulation, IFN γ secretion in response to survivin peptide was enhanced in sTCR⁺CD19.28-OX40⁺ T cells compared with sTCR⁺ T cells (*P* < 0.05), as measured by ELISpot. Conversely, IFN γ secretion by sTCR⁺CD19.28⁺ T cells was decreased compared with NT controls at day 30 (Fig. 1D). Corresponding results were obtained using ELISAs measuring total IFN γ in coculture supernatants in response to TCR stimulation (*P* < 0.01; Fig. 1E). The decrease in IFN γ secretion by sTCR⁺CD19.28⁺ T cells was associated with increased T-cell death between days 20 and 30 resulting in failure to expand (Fig. 1C). Because of poor cytokine release in response to TCR antigen stimulation of CoCAR1-modified sTCR⁺ T cells and increased cell death, further experiments were not performed with this construct. The distribution of effector and memory cells was determined in T cells transduced with CoCAR2 and CoCAR3 constructs and was not significantly different compared with control cells by day 30 (Fig. 1F). To ensure that CoCAR T cells did not kill CD19⁺ target cells, we performed a ⁵¹Cr-release assay with CoCAR⁺ T cells (single-transduced without TCR specificity) compared with conventional CD19-CAR T cells and confirmed lack of cytotoxic activity against CD19⁺ B cells through CoCAR3 (Fig. 1G).

CoCAR3 costimulation amplifies sequential killing activity of sTCR⁺ T cells

To evaluate whether expression of the CoCAR2 and CoCAR3 enhanced antitumor function of sTCR⁺ T cells, we *in vitro* challenged engineered T cells or controls up to eight times with BV173 leukemia cells that present both the cognate survivin peptide and CD19 (Fig. 2A and B). T cells were rechallenged every 3 to 4 days until they were no longer able to eliminate the tumor cells. As expected, NT and

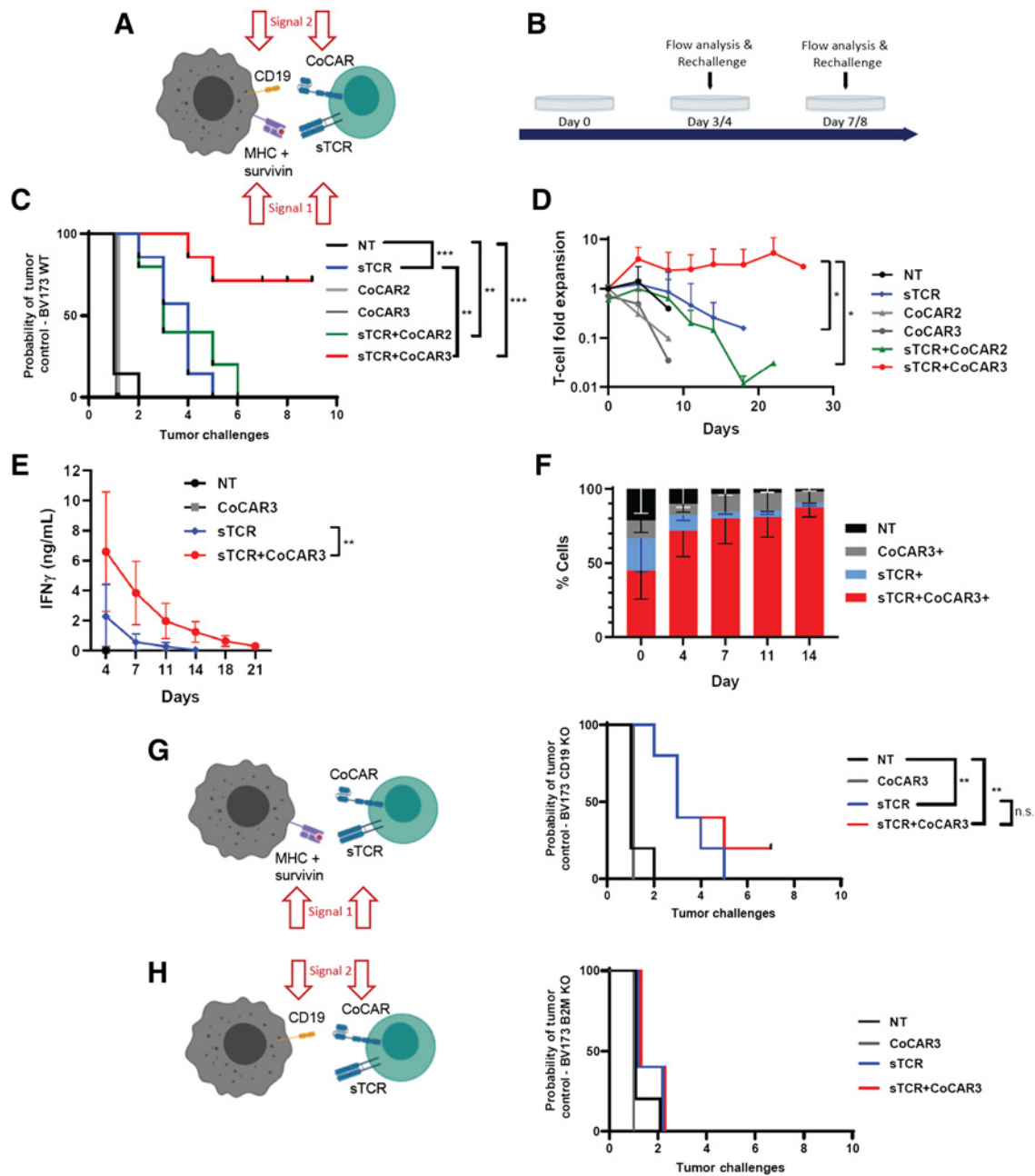


Figure 2.

Costimulation through CoCAR3 enhances the sequential killing activity of sTCR⁺CoCAR3⁺ T cells in an HLA class I- and CD19-restricted manner. **A**, Schematic of T-cell and tumor cell interaction in cocultures. **B**, Timeline and schematic of serial coculture experiment (showing first three timepoints). T cells and tumor cells were cocultured every 3–4 days at an E:T ratio of 1:5 up to eight times. **C**, Tumor cell elimination in serial cocultures ($n = 7$). Marks indicate the time of coculture failure with tumor outgrowth. **D**, T-cell expansion in serial cocultures ($n = 7$). **E**, IFN γ ELISA of coculture supernatants collected 24 hours after each tumor challenge ($n = 5$). **F**, T-cell fractions over time during serial cocultures ($n = 5$). **G**, Schematic of tumor cell and T-cell interaction in coculture with BV173 CD19-KO cells (left). BV173 CD19-KO cell expansion during serial coculture (right). Each line represents one donor ($n = 5$). **H**, Schematic of tumor cell and T-cell interaction in coculture with BV173 B2M-KO cells (left). BV173 B2M-KO expansion during serial coculture (right). Each line represents one donor ($n = 5$). Statistical significance was determined by log-rank test (**C**, **G**), ANOVA (area under the curve; **D**), Welch t test (area under the curve; **E**), paired t test of day 0 versus day 14 (**F**), *, $P < 0.05$; **, $P < 0.01$. **D–F**, mean \pm SD; “ n ” denotes the number of individual healthy donors.

CoCAR⁺ T cells were unable to kill tumor cells (Fig. 2C), whereas sTCR⁺ T cells killed tumor cells for a median of three challenges, with subsequent outgrowth of tumor cells. In contrast, sTCR⁺CoCAR3⁺ T cells extended antitumor activity by a median of four challenges ($P <$

0.01); cells from 5/7 donors eliminated tumor cells for all eight rounds of tumor challenges. Sequential tumor killing activity was associated with increased expansion of sTCR⁺CoCAR3⁺ T cells compared with sTCR⁺ T cells ($P < 0.05$, Fig. 2D). sTCR⁺CoCAR2⁺ T cells did not

improve antitumor activity compared with sTCR⁺ T cells (Fig. 2C), and most T cells died over the course of the coculture (Fig. 2D). Thus, incorporation of CoCAR3, but not CoCAR2, improved sTCR⁺ T-cell sequential killing. Therefore, for the remaining experiments, we eliminated CoCAR2 and continued with CoCAR3 in subsequent sections.

To determine whether CoCAR3 also increased cytokine production by stimulated T cells, we harvested coculture supernatants 24 hours after each tumor rechallenge and measured IFN γ by ELISA. IFN γ secretion was consistently higher in sTCR⁺CoCAR3⁺ T cells compared with sTCR⁺ T cells across all timepoints ($P = 0.0041$; Fig. 2E). CoCAR3 did not induce significant differences in the memory phenotype nor differences in expression of the exhaustion markers TIM-3, LAG3, and PD-1 after the initial two rounds of coculture (Supplementary Fig. S1). In cocultures over time, double-transduced T cells were enriched in the sTCR⁺CoCAR3⁺ T-cell population, with 46.4% ($\pm 18.8\%$) at baseline to 87.8% ($\pm 6.2\%$) by day 14 ($P < 0.01$, Fig. 2F). These results confirmed that double-transduced T cells had a proliferative advantage during serial tumor challenge.

To validate antigen-specific activity of both sTCR and CoCAR3 constructs, we performed sequential cocultures with CD19-KO (lacking the CoCAR antigen) or B2M-KO (unable to present the survivin peptide) BV173 cells. In cocultures with CD19-KO BV173 cells, no difference in the duration of tumor control of sTCR⁺ and sTCR⁺CoCAR3⁺ T cells was observed, indicating absent or minimal background activity of the CoCAR3 in the absence of CD19 antigen (Fig. 2G). In cocultures with B2M-KO BV173 cells, antitumor activity was completely abrogated (Fig. 2H), confirming that, despite high CD19 expression on the target cells, the CoCAR3 has no effect on tumor killing in the absence of signaling through the class I-restricted sTCR.

CoCAR3 increases expression of immunostimulatory pathways upon tumor challenge

To investigate the pathways activated upon CoCAR3 ligation in sTCR⁺CoCAR3⁺ ATCs, we compared the production of T_{H1}/T_{H2} cytokines and cytotoxic granules in coculture supernatants of sTCR⁺CoCAR3⁺ and sTCR⁺ T cells and also performed gene expression analysis on T cells after two challenges with WT BV173 cells (HLA-A*02:01⁺survivin⁺ and CD19⁺). Compared with sTCR⁺ T cells, sTCR⁺CoCAR3⁺ T cells secreted more perforin (3.2-fold increase; $P < 0.05$), granzyme B (11.1-fold increase; $P < 0.05$), TNF α (3.8-fold increase; $P < 0.005$), IFN γ (5.0-fold increase; $P < 0.005$), and GM-CSF (3.7-fold increase; $P < 0.005$; Fig. 3A). IL2, IL4, IL6, and IL10 were low and comparable between conditions [Fig. 3A (IL2); Supplementary Fig. S2]. Consistent with their increased protein levels, IFN γ (IFNG), granzyme B (GZMB), and perforin (PRF1) gene expression was upregulated ($P < 0.05$) in sTCR⁺CoCAR3⁺ compared with sTCR⁺ T cells (Fig. 3B). We also observed increased pathway scores for IL signaling ($P = 0.0378$), T-cell activation ($P = 0.0320$), costimulatory molecules ($P = 0.0288$), and mTOR ($P = 0.0211$) in sTCR⁺CoCAR3⁺ compared with sTCR⁺ T cells (Fig. 3C). Metabolic testing at baseline and after coculture with tumor cells using the seahorse assay showed a trend toward increased spare respiratory capacity in sTCR⁺CoCAR3⁺ over sTCR⁺ T cells after two rounds of coculture (Supplementary Fig. S3), but this difference did not reach statistical significance.

CoCAR3 improves tumor control, including tumors with heterogeneous CD19 expression

Because CD19 (the CoCAR antigen) might be heterogeneously expressed on tumors or provided by normal bystander cells, we

investigated the amount of CD19-positivity required to produce sufficient stimulation through CoCAR3 to enhance antitumor activity. We tested sequential killing ability and cytokine production of sTCR⁺CoCAR3⁺ T cells in a modified coculture assay. By mixing WT with CD19-KO BV173 tumor cells at various ratios, we created tumor target populations with 100%, 75%, 50%, 25%, or 0% CD19⁺ cells (Fig. 4A). With 100%, 75%, and 50% CD19⁺ targets, sTCR⁺CoCAR3⁺ T cells eliminated tumor cells for four additional challenges compared with sTCR⁺ T cells ($P < 0.01$; Fig. 4B). At 25% CD19-positivity, sTCR⁺CoCAR3⁺ T cells still showed a trend toward prolonged tumor elimination in comparison with sTCR⁺ T cells (median increase of 2.5 cocultures; interquartile range, 1 to 4). Consistent with prior coculture results, sTCR⁺ and sTCR⁺CoCAR3⁺ T cells did not differ in their activity against CD19-negative tumor cells, indicating minimal background signaling of the CoCAR.

As expected, the proportion of CD19⁺ cells in culture did not affect IFN γ production by sTCR⁺ T cells (Fig. 4C, left). sTCR⁺CoCAR3⁺ T cells produced similar amounts of IFN γ when 100%, 75%, or 50% of BV173 cells expressed CD19 (100% CD19⁺: 3,278 \pm 1,172 ng/mL, 75%: 2,951 \pm 1,297 ng/mL, 50%: 2,915.9 \pm 1,185 ng/mL). IFN γ concentration decreased when 25% of tumor cells expressed CD19 (1,534.9 \pm 733.0 ng/mL, P not significant vs. 50%, 75% and 100%), but remained 2.4 times higher than in the absence of CD19 (651.3 \pm 473.4 ng/mL; $P < 0.05$).

CoCAR3 enhances the antitumor function of sTCR⁺ T cells in a leukemia model

Next, we evaluated whether CoCAR3 enhanced the *in vivo* antitumor function of sTCR⁺ T cells in our previously established BV173-FFLuc mouse xenograft model (14, 15). Sublethally irradiated mice were injected intravenously with BV173-FFLuc cells, followed 7 days later by a single intravenous injection of 1×10^7 T cells (Fig. 5A). As expected, NT and CoCAR3⁺ T cells failed to control the leukemia, whereas a significant delay in leukemia progression was observed in mice treated with sTCR⁺CoCAR3⁺ compared with sTCR⁺ T cells, and this delay in tumor progression improved overall survival of mice treated with sTCR⁺CoCAR3⁺ over sTCR⁺ T cell-treated mice by a median of 35 days (Fig. 5B and C; $P < 0.01$). We confirmed the improved antitumor efficacy in less established tumors using a lower T-cell dose of 4×10^6 cells administered 1 day after tumor cell injection (Supplementary Fig. S4). At this dose, treatment with sTCR⁺ T cells alone did not extend survival over NT control cells, whereas treatment with sTCR⁺CoCAR3⁺ T cells resulted in improved survival by 11 days ($P < 0.01$).

CoCAR3 accelerates antitumor responses in a xenograft model of EBV lymphoma

To investigate the effect of CoCAR3 costimulation on the function of tumor-specific T cells expressing native TCRs with a broad repertoire, we engineered EBVSTs with the CoCAR3. We achieved a mean transduction efficiency of 60.9% ($\pm 27.3\%$), which remained stable during EBVST expansion (Fig. 6A). The transduction procedure briefly slowed EBVST expansion, but fold expansion was similar to NT EBVSTs after the second stimulation (Fig. 6B). The CoCAR3 increased the frequency of EBV-specific T cells within the EBVSTs by a mean of 2.4-fold (90% confidence interval: 2.4 \pm 1.3) as measured by an IFN γ ELISpot at the end of the first stimulation cycle (S1) in five of six donors (Fig. 6C). Memory phenotype, determined by CD45RO and CCR7 expression, was unaffected by CoCAR3 expression over two stimulations, and a trend toward a higher proportion of CD8⁺ T cells in CoCAR3⁺ EBVSTs after the second stimulation was not statistically

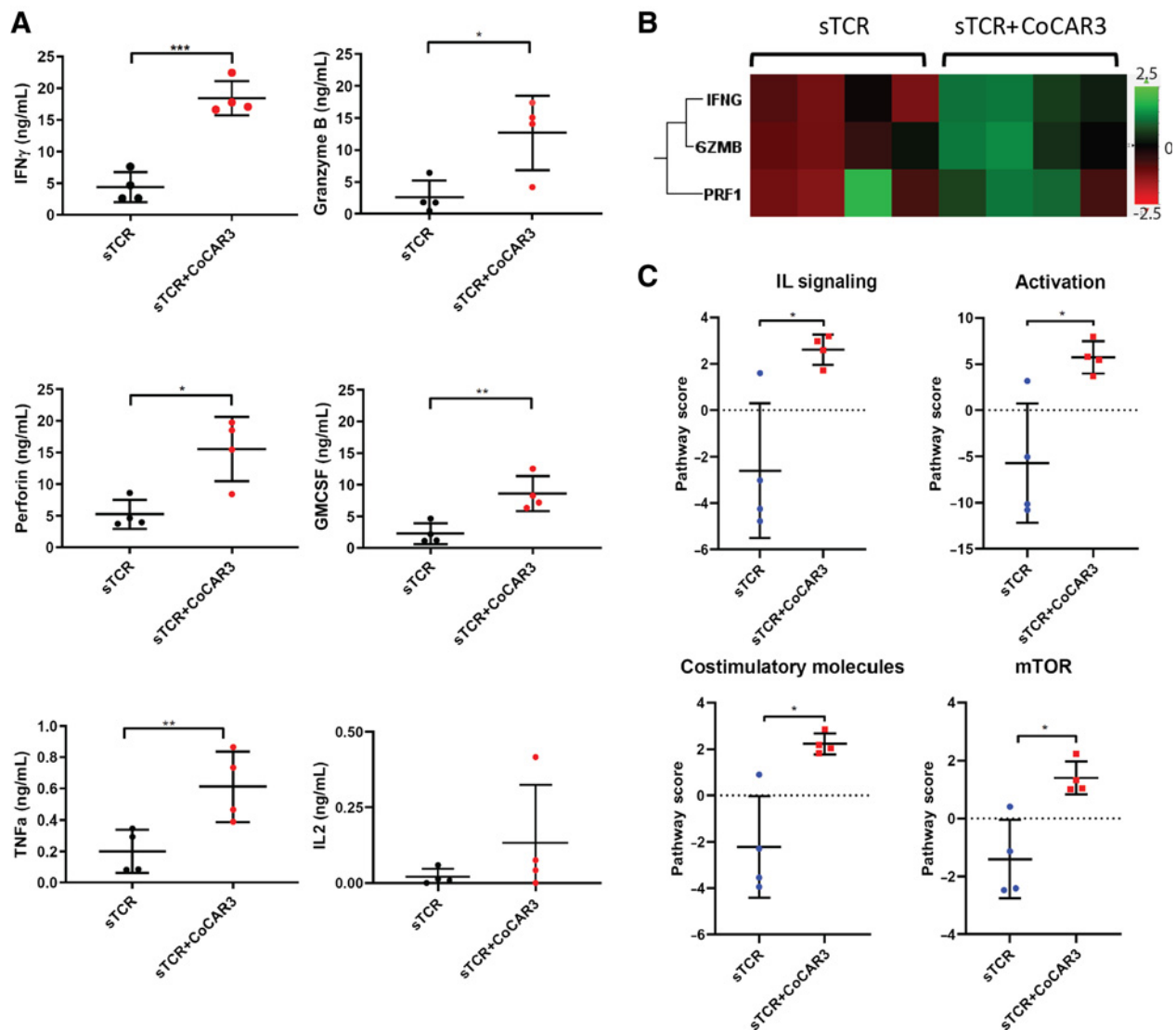


Figure 3.

Immunostimulatory pathways are activated in sTCR⁺CoCAR3⁺ T cells upon sequential tumor challenge. **A**, Detection of IFN γ , perforin, and TNF α in coculture supernatants 24 hours after the second tumor challenge ($n = 4$) as described in **Fig. 2B**. **B** and **C**, RNA expression in engineered T cells 24 hours after second tumor challenge using NanoString (see Materials and Methods). **B**, Heatmap showing genes with significant log₂ fold changes (sTCR⁺ vs. sTCR⁺CoCAR3⁺ T cells, $P < 0.05$; $n = 4$). **C**, Pathway scores for sTCR⁺ and sTCR⁺CoCAR3⁺ T cells as determined by NanoString. **A** and **C**, Statistical significance was determined by paired t test, *, $P < 0.05$; **, $P < 0.01$; ***, $P < 0.005$; mean \pm SD, “ n ” denotes the number of individual healthy donors.

significant (Supplementary Fig. S5). We confirmed lack of bystander killing in a cytotoxicity assay using CoCAR3⁺ EBVSTs as effector cells (NT EBVSTs in the control condition) and an EBV⁺CD19⁺ LCLs as target cells (Supplementary Fig. S6); labeled EBV-negative B cells were not killed, even when mixed with CD19⁺ EBV-LCLs that were targeted and killed by CoCAR3⁺ EBVSTs.

We then evaluated the antitumor activity of engineered CoCAR3⁺ EBVSTs in an autologous EBV-LCL xenograft mouse model. After EBV-LCL tumors were injected subcutaneously and established, NSG mice were injected intravenously with 5×10^6 FFLuc-engineered EBVSTs or CoCAR3⁺ EBVSTs or irrelevant VSTs specific for CMV. T-cell expansion was monitored by BLI (**Fig. 6D**). CoCAR3⁺ EBVSTs expanded more rapidly than NT-EBVSTs (**Fig. 6E and F**), which in turn correlated with more rapid tumor control (**Fig. 6G**). The peak of

EBVST expansion, measured by BLI signal at the tumor site, occurred on day 9 after infusion of CoCAR3⁺ EBVSTs and at the time was 7.3-fold higher than for EBVSTs (BLI total flux day 9: 1.7 ± 1.1 vs. $12 \pm 1.6 \times 10^9$ p/s; $P < 0.0001$). The increased EBVST expansion preceded a reduction in tumor size, which was 77.1% smaller in CoCAR3⁺ EBVST compared with EBVST-treated mice on day 13 (0.81 ± 0.25 vs. 0.13 ± 0.12 cm³; $P = 0.005$; **Fig. 6G**, right).

Discussion

In this study, we showed that engineered costimulation through a CD19.28-OX40 CoCAR (CoCAR3) enhanced the antitumor activity of T cells with both native and tTCRs *in vitro* and *in vivo* in two different xenograft models of leukemia and lymphoma. CoCAR3-

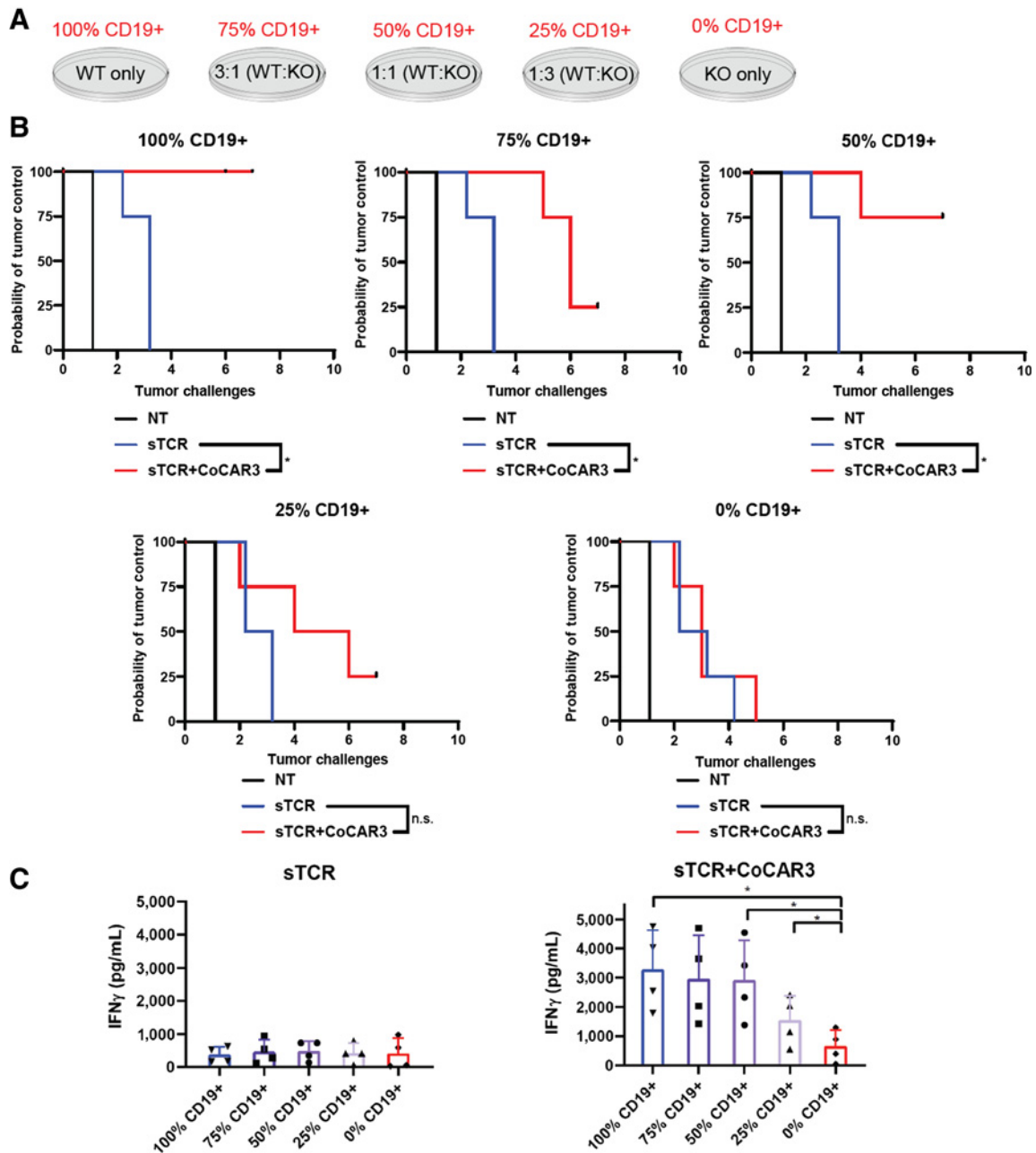


Figure 4.

CoCAR3 maintains immune-stimulatory effects in tumors with heterogeneous CD19 expression. **A**, Schematic of mixed tumor cell population cocultures. BV173 WT cells were mixed at the indicated ratios with BV173 CD19-KO cells to mimic various CD19 expression in the overall population. The mixed tumor cells were used in a serial coculture as described in **Fig. 2B**. T cells were rechallenged with the same tumor mixture every 3–4 days for a total of eight challenges. **B**, Tumor cell expansion during serial cocultures ($n = 4$). **C**, Coculture supernatants were harvested 24 hours after the second tumor challenge and analyzed for IFN γ by ELISA, mean \pm SD. Statistical significance was determined by ANOVA with Tukey multiple comparisons test, *, $P < 0.05$; **, $P < 0.01$; “n” denotes the number of individual healthy donors.

mediated costimulation improved the antitumor activity of T cells, even when targeting tumors with heterogeneous CD19 expression. Our approach provides the proof of concept that costimulation with a CoCAR can specifically enhance antitumor function of native and tTCR T cells.

Engineering strategies to provide local costimulation or cytokine signals to T cells within the TME have focused mostly on converting

inhibitory immune checkpoint (25) or cytokine signals (26) into immune-stimulatory outputs (recently reviewed in ref. 11) or by direct modification of tTCRs (27). Preclinical evaluation of CoCARs has investigated their ability to mitigate the toxicity of CAR T-cell therapies, in which two different target antigens are recognized simultaneously by two independent CARs, termed a “split CAR” system. In these systems, a first-generation CAR provides CD3 ζ signaling and the

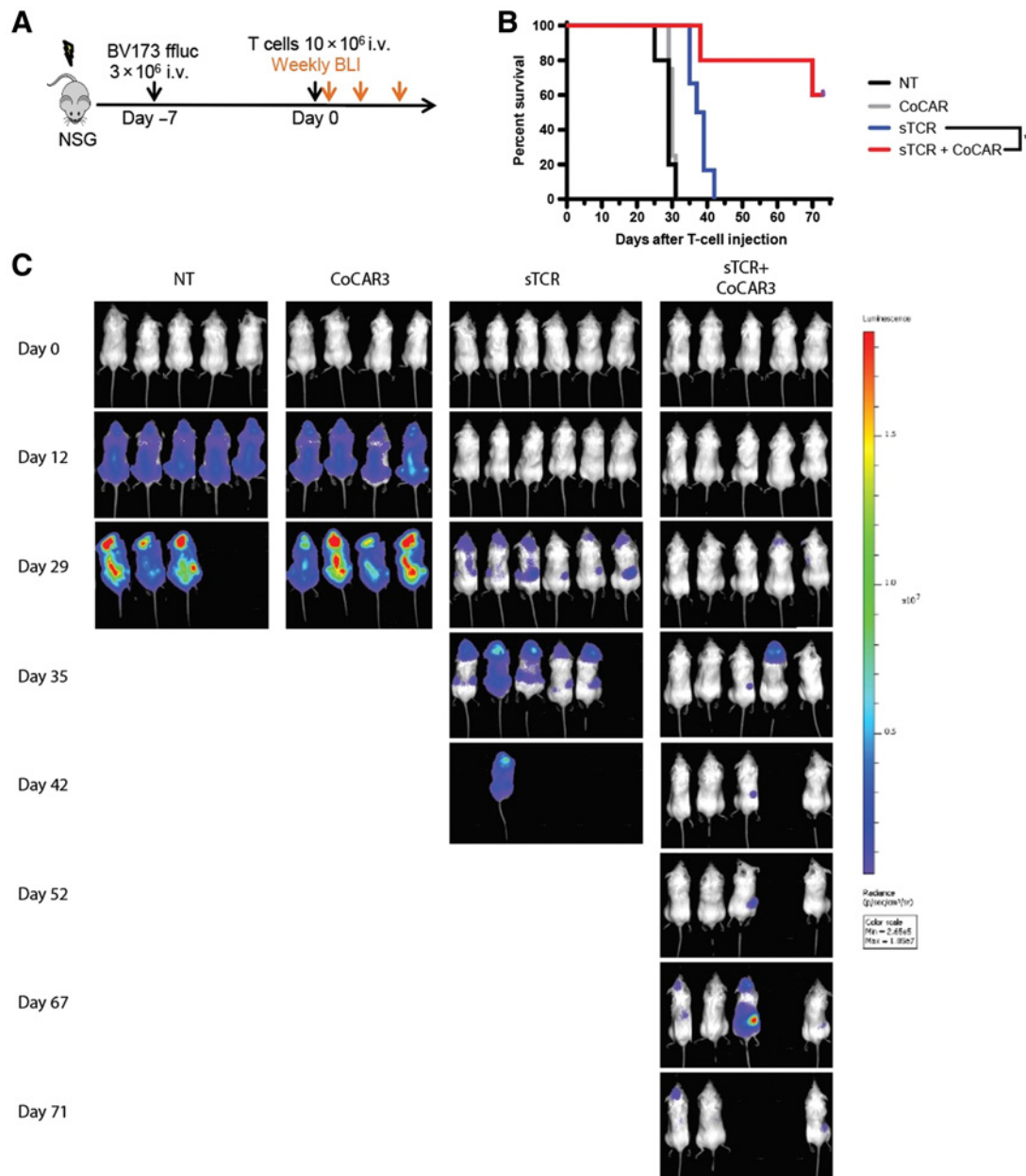


Figure 5. CoCAR3 activation enhances the antitumor function of sTCR⁺ T cells *in vivo*. **A**, Schematic of mouse model. NSG mice were sublethally irradiated then injected with BV173-ffluc cells. Seven days later, T cells expressing CoCAR3, sTCR, or sTCR⁺CoCAR3 were injected. Mice treated with NT cells were used as controls. Mice were monitored for tumor progression weekly. BLI, bioluminescent Imaging. **B**, Survival of mice. **C**, Bioluminescent images showing tumor signal over time. Statistical significance was determined by log-rank (Mantel-Cox), *, *P* < 0.01. NT *n* = 5, CoCAR3 *n* = 4, sTCR *n* = 6, and sTCR+CoCAR3 *n* = 5.

CoCAR exclusively provides costimulation (28, 29) with the goal to modulate cytotoxicity and potential on-target/off-tumor toxicity of the CAR. However, the immune-enhancing effects of CoCARs in combination with native or tTCRs had not yet been explored.

We initially evaluated three different costimulatory endodomains, (i) CD28, (ii) 41BB, and (iii) CD28 combined with OX40, selected on the basis of their different biology. Although standard CD19.28.ζ CAR T cells expand and contract rapidly after infusion in patients (30), CD19.41BB.ζ CAR T cells are known for slightly slower onset of action

and longer-term persistence (31–33). The CD28-OX40 endodomain has previously been validated preclinically in CAR T cells with a range of different antigen specificities (34–39). In a comparison of 12 different costimulatory molecules, OX40 was shown to confer the greatest benefit to 41BBζ.CAR T cells, increasing T-cell proliferation, cytotoxicity, and antitumor activity (40). In our experiments, the CD19.28-OX40 CoCAR3 outperformed the CD19.28 and the CD19.41BB CoCAR constructs, with increased proliferation compared with CD19.28 and superior performance in sequential

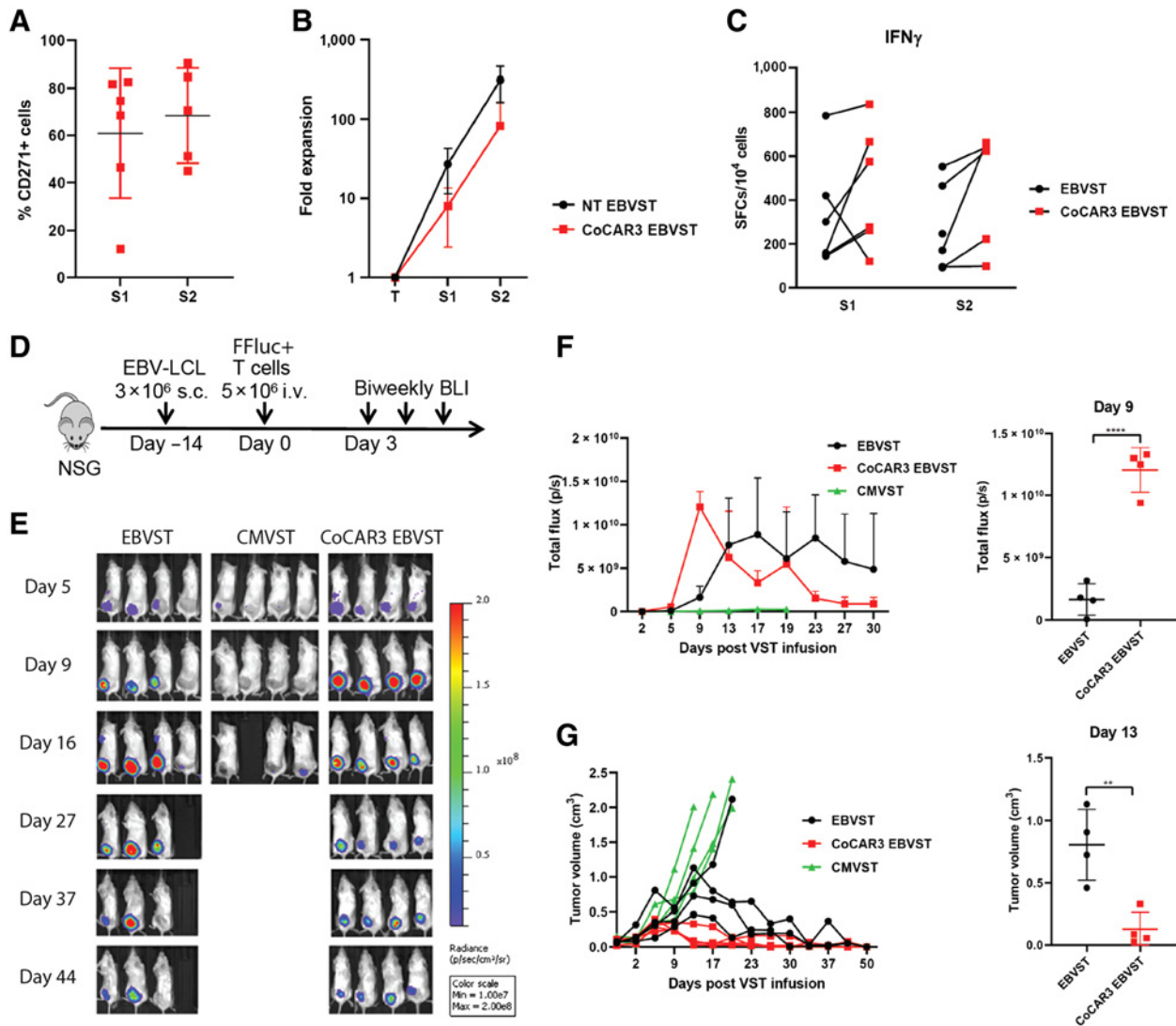


Figure 6. CoCAR3 accelerates clearance of EBV⁺ lymphoma *in vivo*. **A**, Transduction efficiency of CoCAR3⁺ EBVSTs at the end of S1 and S2. S1 = first stimulation. S2 = second stimulation. **B**, Fold EBVST expansion following transduction on day 3 (*n* = 6 S1; *n* = 5 S2). NT: nontransduced. **C**, Frequency of IFN γ spot-forming cells (SFC) in response to EBV-pepmix at S1 and S2 by ELISpot (*n* = 6). Connected points indicate paired samples. **D**, Schema of *in vivo* xenograft model. NSG mice were subcutaneously injected with EBV-LCL tumor cells. Two weeks later, ffluc⁺ EBVSTs (NT or CoCAR3⁺) were injected into the mice. Ffluc⁺ CMVSTs were used as controls. BLI, bioluminescent Imaging. **E**, BLI of virus-specific T cell (VST) expansion over time in individual mice with established subcutaneous EBV lymphomas (*n* = 4). **F**, Left: Summary of BLI (p/s) of VSTs (*n* = 4). Right: Day 9 BLI summary comparing EBVST and CoCAR3⁺ EBVST signal intensity (*n* = 4). **G**, Left: LCL tumor volume (cm³). Each line represents one mouse (*n* = 4/group). Right: Day 13 summary of tumor volume in mice treated with EBVSTs or CoCAR3⁺ EBVSTs (*n* = 4). (**A**, **B**, **F**, **G**) mean \pm SD. **F** and **G**, Statistical significance was determined by Student *t* test, **, *P* < 0.01; ****, *P* < 0.0001; “*n*” denotes the number of individual healthy donors.

tumor killing assays. Because our CoCAR constructs exerted minimal antigen-independent activity, we hypothesize that minimal baseline signaling of the CD19.28-OX40 CoCAR3 may avoid the effects of tonic signaling that results in T-cell exhaustion, as observed with CD28-OX40 ζ in the context of a GD2-CAR (37), while maintaining the beneficial effects of OX40 on T-cell function and persistence (40).

We selected CD19 as an extensively characterized and clinically validated CAR target that could provide the following advantages: (i) CD19 is expressed on both lymphoid malignancies and normal B cells; (ii) normal CD19⁺ lymphocytes are abundant throughout the

blood and lymphoid tissues and are easily encountered by adoptively transferred T cells; (iii) B cells can provide additional costimulation as professional antigen-presenting cells if they receive signals from activated T cells; and (iv) activated B cells are often recruited to tumors with proinflammatory environments. Therefore, the CD19-CoCAR may allow for activation of the CoCAR by the tumor itself *in cis* or *in trans* by B cells in lymph nodes or the TME.

Our results demonstrate that CoCAR3 enhanced the potency of tumor-specific native and tTCR T cells when encountering CD19 on as few as 25% target cells. Because the CoCAR is not cytotoxic, it should

not drive antigen escape, but if antigen escape did occur, or if the CoCAR target antigen was expressed in only a subset of cells, its beneficial effect would therefore not be diminished. Possible explanations for this observation are that (i) CoCAR activation by CD19 *in cis* leads to sustained CD28-OX40 activation beyond the first target cell recognition and killing; (ii) CoCAR3-engineered T cells produce cytokines, proliferate, and then encounter and kill additional target cells, even in the absence of CD19 expression; and (iii) provision of CD19 *in trans* may activate CoCAR-mediated signaling and enhance target cell killing through the TCR. However, the spatio-temporal sequence of events could not be fully elucidated in our experimental system.

We investigated our CoCAR3 approach in two different murine xenograft models, one targeting a poorly immunogenic, aggressive acute leukemia using a tTCR, and the other targeting highly immunogenic EBV⁺ LCLs using polyclonal EBVSTs expressing nTCRs. In both models, CoCAR3 enhanced the antitumor activity of the T cells, even though the models differ significantly in several aspects. The tTCR has low affinity, is HLA class I-restricted, and is CD8-dependent. By contrast, polyclonal nTCRs in EBVSTs are, in general, of high affinity, as they are targeting foreign viral antigens (41), and comprise a mixture of CD4⁺ and CD8⁺ T cells. Unlike most EBV⁺ lymphomas and other EBV⁺ cancers, EBV⁺ LCLs are highly immunogenic and express high levels of costimulatory ligands that may mask the full potential of engineered costimulation through the CoCAR3. In our LCL xenograft model, we observed more rapid initial expansion, followed by more rapid contraction of the CoCAR-modified EBVSTs, as tumors were controlled. At the time the T-cell signal decreased, all tumors had resolved by palpation, and none of the mice experienced tumor recurrence, indicating that the lack of EBV antigen (signal 1) and CD19 antigen (signal 2) following rapid tumor clearance resulted in the decline in T-cell numbers.

Finally, we performed gene expression analysis of sTCR⁺CoCAR3⁺ T cells upon tumor challenge to determine changes conferred by the CoCAR in response to targeted tumors. We found upregulation of genes associated with T-cell activation, costimulation, and cytokine signaling, indicating that several pathways contribute to the observed functional changes. The upregulation of these genes was associated with increased granzyme B, perforin, IFN γ , and other cytokines and enzymes, which may confer increased antitumor activity to CoCAR-modified cells. Our group and others have previously investigated the interactions between CAR signaling and TCR signaling in VSTs. The combination of signaling through both the CAR and through the native/tTCR can produce excessive CD3 ζ signaling, which can in turn produce activation-induced cell death (AICD; refs. 42, 43). The CoCAR approach avoids this excessive ζ signaling seen with conventional CARs, thus decreasing the risk of AICD.

We consider our proposed combination of TCR targeting with CoCAR costimulation to be a model system that could be adapted to target other cancer types, either by targeting tumors with high B-cell numbers in the TME or by changing the antigen-targeting domain to an alternative antigen relevant to the targeted tumor. The lack of costimulatory ligand expression in the TME is particularly problematic in solid tumors. Accordingly, durable clinical benefit after TIL therapy or tTCR T-cell therapies in solid tumors has only been achieved in a minority of patients treated (6, 7, 9), indicating a major need to develop strategies that deliver immune stimulation for TCR-based ACT. Additional provision of CoCAR-modified T cells with supplemented

or engineered cytokine signaling could further enhance their efficacy by completing the three-signal requirement of T-cell activation (44).

In summary, we provide a proof-of-concept study that engineered costimulation with a CoCAR can significantly enhance the antitumor activity of TCR-based cell therapies, with both native and tTCRs, while sparing normal cells that express the CoCAR-targeted antigen. Our novel approach may be extended to other antigens with the goal to provide tumor- and TME-specific costimulation.

Authors' Disclosures

B. Omer reports grants from Gabrielle's Angel Foundation, NIH, Cancer Prevention and Research Institute of Texas, and Texas Children's Cancer Center K12 during the conduct of the study. C. DeRenzo reports grants from the Rally Foundation for Childhood Cancer Research, The Truth 365, the Sarcoma Foundation of America, and the NIH grant K12CA0904335 during the conduct of the study. S. Gottschalk reports other support from TESSA Therapeutics, Immatics, Catamaran Bio, TIDAL, and Nektar Therapeutics outside the submitted work; in addition, S. Gottschalk has multiple patents in the field of engineered T-cell therapies pending. C. Arber reports grants from Cancer Prevention & Research Institute of Texas during the conduct of the study; in addition, C. Arber has a patent for Survivin-specific T cell receptor targeting tumor but not T cells issued, a patent for Reprogramming CD4 T cells into cytotoxic CD8 cells by forced expression of CD8ab and class I-restricted T-cell receptors issued, licensed, and with royalties paid from Immatics, and a patent for transgenic c-MPL provides ligand-dependent costimulation and cytokine signals to TCR-engineered T cells pending. C.M. Rooney reports grants from NIH-NCI during the conduct of the study; grants and personal fees from Tessa Therapeutics; personal fees from Allovir, Marker Therapeutics, Bellicum Pharmaceuticals, Allogene, Abintus, Bluebird Bio, Memgen, TScan, Turnstone Biologics, and Walking Fish outside the submitted work. No disclosures were reported by the other authors.

Authors' Contributions

B. Omer: Conceptualization, resources, data curation, supervision, funding acquisition, validation, investigation, methodology, writing—original draft, project administration, writing—review and editing. **M.G. Cardenas:** Data curation, formal analysis, investigation, methodology, writing—original draft, writing—review and editing. **T. Pfeiffer:** Data curation, formal analysis, writing—review and editing. **R. Daum:** Data curation, writing—review and editing. **M. Huynh:** Data curation, writing—review and editing. **S. Sharma:** Data curation, writing—review and editing. **N. Nourae:** Data curation, methodology, writing—review and editing. **C. Xie:** Data curation. **C. Tat:** Data curation. **S. Perconti:** Data curation, writing—review and editing. **S. Van Pelt:** Data curation, supervision, writing—review and editing. **L. Scherer:** Data curation, writing—review and editing. **C. DeRenzo:** Methodology, writing—review and editing. **T. Shum:** Data curation, methodology, writing—review and editing. **S. Gottschalk:** Conceptualization, methodology, writing—review and editing. **C. Arber:** Conceptualization, resources, formal analysis, funding acquisition, validation, methodology, writing—original draft, project administration, writing—review and editing. **C.M. Rooney:** Conceptualization, resources, formal analysis, supervision, funding acquisition, validation, methodology, writing—original draft, project administration, writing—review and editing.

Acknowledgments

This work is supported by NIH SPORE in lymphoma (5P50CA126752; B. Omer, C.M. Rooney), Gabrielle's Angels Foundation for Cancer Research (B. Omer), Texas Children's Cancer Center K12 (K12CA090433; B. Omer), Cancer Prevention & Research Institute of Texas (CPRIT IIRA RP160345; C. Arber, M.G. Cardenas) and Sharon Levin Fund.

The costs of publication of this article were defrayed in part by the payment of page charges. This article must therefore be hereby marked *advertisement* in accordance with 18 U.S.C. Section 1734 solely to indicate this fact.

Received April 22, 2021; revised November 11, 2021; accepted February 11, 2022; published first February 16, 2022.

References

- Haen SP, Loffler MW, Rammensee HG, Brossart P. Towards new horizons: characterization, classification and implications of the tumour antigenic repertoire. *Nat Rev Clin Oncol* 2020;17:595–610.
- Heslop HE, Slobod KS, Pule MA, Hale GA, Rousseau A, Smith CA, et al. Long-term outcome of EBV-specific T-cell infusions to prevent or treat EBV-related lymphoproliferative disease in transplant recipients. *Blood* 2010;115:925–35.
- Haque T, Wilkie GM, Jones MM, Higgins CD, Urquhart G, Wingate P, et al. Allogeneic cytotoxic T-cell therapy for EBV-positive posttransplantation lymphoproliferative disease: results of a phase 2 multicenter clinical trial. *Blood* 2007;110:1123–31.
- Prockop S, Doubrovina E, Suser S, Heller G, Barker J, Dahi P, et al. Off-the-shelf EBV-specific T cell immunotherapy for rituximab-refractory EBV-associated lymphoma following transplantation. *J Clin Invest* 2020;130:733–47.
- Dafni U, Michielin O, Lluemas SM, Tsourti Z, Polydoropoulou V, Karlis D, et al. Efficacy of adoptive therapy with tumor-infiltrating lymphocytes and recombinant interleukin-2 in advanced cutaneous melanoma: a systematic review and meta-analysis. *Ann Oncol* 2019;30:1902–13.
- Tran E, Robbins PF, Lu YC, Prickett TD, Gartner JJ, Jia L, et al. T-cell transfer therapy targeting mutant KRAS in cancer. *N Engl J Med* 2016;375:2255–62.
- Morgan RA, Dudley ME, Wunderlich JR, Hughes MS, Yang JC, Sherry RM, et al. Cancer regression in patients after transfer of genetically engineered lymphocytes. *Science* 2006;314:126–9.
- Rapoport AP, Stadtmauer EA, Binder-Scholl GK, Goloubeva O, Vogl DT, Lacey SF, et al. NY-ESO-1-specific TCR-engineered T cells mediate sustained antigen-specific antitumor effects in myeloma. *Nat Med* 2015;21:914–21.
- D'Angelo SP, Melchiori L, Merchant MS, Bernstein D, Glod J, Kaplan R, et al. Antitumor activity associated with prolonged persistence of adoptively transferred NY-ESO-1 (c259)T cells in synovial sarcoma. *Cancer Discov* 2018;8:944–57.
- Chapuis AG, Egan DN, Bar M, Schmitt TM, McAfee MS, Paulson KG, et al. T cell receptor gene therapy targeting WT1 prevents acute myeloid leukemia relapse post-transplant. *Nat Med* 2019;25:1064–72.
- Rath JA, Arber C. Engineering strategies to enhance TCR-based adoptive T cell therapy. *Cells* 2020;9:1485.
- Fesnak AD, June CH, Levine BL. Engineered T cells: the promise and challenges of cancer immunotherapy. *Nat Rev Cancer* 2016;16:566–81.
- Savoldo B, Ramos CA, Liu E, Mims MP, Keating MJ, Carrum G, et al. CD28 costimulation improves expansion and persistence of chimeric antigen receptor-modified T cells in lymphoma patients. *J Clin Invest* 2011;121:1822–6.
- Arber C, Feng X, Abhyankar H, Romero E, Wu MF, Heslop HE, et al. Survivin-specific T cell receptor targets tumor but not T cells. *J Clin Invest* 2015;125:157–68.
- Nishimura CD, Brenner DA, Mukherjee M, Hirsch RA, Ott L, Wu MF, et al. c-MPL provides tumor-targeted T-cell receptor-transgenic T cells with costimulation and cytokine signals. *Blood* 2017;130:2739–49.
- Rath JA, Bajwa G, Carreres B, Hoyer E, Gruber I, Martinez-Paniagua MA, et al. Single-cell transcriptomics identifies multiple pathways underlying antitumor function of TCR- and CD8alpha-engineered human CD4(+) T cells. *Sci Adv* 2020;6:eaz7809.
- Bollard CM, Gottschalk S, Torrano V, Diouf O, Ku S, Hazrat Y, et al. Sustained complete responses in patients with lymphoma receiving autologous cytotoxic T lymphocytes targeting Epstein-Barr virus latent membrane proteins. *J Clin Oncol* 2014;32:798–808.
- Gundry MC, Brunetti L, Lin A, Mayle AE, Kitano A, Wagner D, et al. Highly efficient genome editing of murine and human hematopoietic progenitor cells by CRISPR/Cas9. *Cell Rep* 2016;17:1453–61.
- Huang S, Stupack D, Liu A, Cheres D, Nemerow GR. Cell growth and matrix invasion of EBV-immortalized human B lymphocytes is regulated by expression of alpha(v) integrins. *Oncogene* 2000;19:1915–23.
- Kochenderfer JN, Feldman SA, Zhao Y, Xu H, Black MA, Morgan RA, et al. Construction and preclinical evaluation of an anti-CD19 chimeric antigen receptor. *J Immunother* 2009;32:689–702.
- Prinzling B, Schreiner P, Bell M, Fan Y, Krenziute G, Gottschalk S. MyD88/CD40 signaling retains CAR T cells in a less differentiated state. *JCI Insight* 2020;5:e136093.
- Gerdemann U, Vera JF, Rooney CM, Leen AM. Generation of multivirus-specific T cells to prevent/treat viral infections after allogeneic hematopoietic stem cell transplant. *J Vis Exp* 2011;51:2736.
- Sharma S, Rooney CM, Parikh K. Depletion of CD45RA-positive cells removes an inhibitory component that potentiates the reactivation of EBV-specific T-cells from lymphoma patients. *Mol Ther* 2019;27:457.
- Sun J, Huye LE, Lapteva N, Mamonkin M, Hiregange M, Ballard B, et al. Early transduction produces highly functional chimeric antigen receptor-modified virus-specific T-cells with central memory markers: a Production Assistant for Cell Therapy (PACT) translational application. *J Immunother Cancer* 2015;3:5.
- Ankri C, Shamalov K, Horovitz-Fried M, Mauer S, Cohen CJ. Human T cells engineered to express a programmed death 1/28 costimulatory retargeting molecule display enhanced antitumor activity. *J Immunol* 2013;191:4121–9.
- Leen AM, Sukumaran S, Watanabe N, Mohammed S, Keirnan J, Yanagisawa R, et al. Reversal of tumor immune inhibition using a chimeric cytokine receptor. *Mol Ther* 2014;22:1211–20.
- Govers C, Sebestyen Z, Roszik J, van Brakel M, Berrevoets C, Szoor A, et al. TCRs genetically linked to CD28 and CD3epsilon do not mispair with endogenous TCR chains and mediate enhanced T cell persistence and anti-melanoma activity. *J Immunol* 2014;193:5315–26.
- Kloss CC, Condomines M, Cartellieri M, Bachmann M, Sadelain M. Combinatorial antigen recognition with balanced signaling promotes selective tumor eradication by engineered T cells. *Nat Biotechnol* 2013;31:71–5.
- Lanitis E, Poussin M, Klattenhoff AW, Song D, Sandaltzopoulos R, June CH, et al. Chimeric antigen receptor T Cells with dissociated signaling domains exhibit focused antitumor activity with reduced potential for toxicity *in vivo*. *Cancer Immunol Res* 2013;1:43–53.
- Neelapu SS, Locke FL, Bartlett NL, Lekakis LJ, Miklos DB, Jacobson CA, et al. Axicabtagene ciloleucel CAR T-cell therapy in refractory large B-cell lymphoma. *N Engl J Med* 2017;377:2531–44.
- Maude SL, Laetsch TW, Buechner J, Rives S, Boyer M, Bittencourt H, et al. Tisagenlecleucel in children and young adults with B-cell lymphoblastic leukemia. *N Engl J Med* 2018;378:439–48.
- Kawalekar OU, O'Connor RS, Fraietta JA, Guo L, McGittigan SE, Posey AD Jr, et al. Distinct signaling of coreceptors regulates specific metabolism pathways and impacts memory development in CAR T cells. *Immunity* 2016;44:380–90.
- Salter AI, Ivey RG, Kennedy JJ, Voillet V, Rajan A, Alderman EJ, et al. Phosphoproteomic analysis of chimeric antigen receptor signaling reveals kinetic and quantitative differences that affect cell function. *Sci Signal* 2018;11:eaat6753.
- Pule MA, Straathof KC, Dotti G, Heslop HE, Rooney CM, Brenner MK. A chimeric T cell antigen receptor that augments cytokine release and supports clonal expansion of primary human T cells. *Mol Ther* 2005;12:933–41.
- Quintarelli C, Orlando D, Boffa I, Guercio M, Polito VA, Petretto A, et al. Choice of costimulatory domains and of cytokines determines CAR T-cell activity in neuroblastoma. *Oncimmunology* 2018;7:e1433518.
- Lee L, Draper B, Chaplin N, Philip B, Chin M, Galas-Filipowicz D, et al. An APRIL-based chimeric antigen receptor for dual targeting of BCMA and TACI in multiple myeloma. *Blood* 2018;131:746–58.
- Long AH, Haso WM, Shern JF, Wanhainen KM, Murgai M, Ingaramo M, et al. 4-1BB costimulation ameliorates T cell exhaustion induced by tonic signaling of chimeric antigen receptors. *Nat Med* 2015;21:581–90.
- Heczey A, Louis CU, Savoldo B, Dakhova O, Durett A, Grilley B, et al. CAR T cells administered in combination with lymphodepletion and PD-1 inhibition to patients with neuroblastoma. *Mol Ther* 2017;25:2214–24.
- Guercio M, Orlando D, Di Cecca S, Sinibaldi M, Boffa I, Caruso S, et al. CD28. OX40 co-stimulatory combination is associated with long *in vivo* persistence and high activity of CAR-CD30 T-cells. *Haematologica* 2021;106:987–99.
- Zhang H, Li F, Cao J, Wang X, Cheng H, Qi K, et al. A chimeric antigen receptor with antigen-independent OX40 signaling mediates potent antitumor activity. *Sci Transl Med* 2021;13:eaba7308.
- Aleksic M, Liddy N, Molloy PE, Pumphrey N, Vuidepot A, Chang KM, et al. Different affinity windows for virus and cancer-specific T-cell receptors: implications for therapeutic strategies. *Eur J Immunol* 2012;42:3174–9.
- Brocker T, Karjalainen K. Signals through T cell receptor-zeta chain alone are insufficient to prime resting T lymphocytes. *J Exp Med* 1995;181:1653–9.
- Omer B, Castillo PA, Tashiro H, Shum T, Huynh MTA, Cardenas M, et al. Chimeric antigen receptor signaling domains differentially regulate proliferation and native T cell receptor function in virus-specific T cells. *Front Med* 2018;5:343.
- Shum T, Omer B, Tashiro H, Kruse RL, Wagner DL, Parikh K, et al. Constitutive signaling from an engineered IL7 receptor promotes durable tumor elimination by tumor-redirectioned T cells. *Cancer Discov* 2017;7:1238–47.